

Evidence for a Cooper minimum in the photoionization dynamics of the NO D²Σ⁺ state

Hongkun Park, Richard N. Zare

Department of Chemistry, Stanford University, Stanford, CA 94305, USA

Received 8 March 1994; in final form 26 May 1994

Abstract

Rotationally resolved photoelectron angular distributions are reported for the two-color, two-photon process NO X²Π ($v_x=0$, $J_x=17.5$) + $h\nu_1 \rightarrow$ NO D²Σ⁺ ($v=0$, $N=18$) + $h\nu_2 \rightarrow$ NO⁺ X¹Σ⁺ ($v^+=0$, N^+) + e⁻. The positive and negative ΔN transitions ($\Delta N=N^+-N$) for the same value of $|\Delta N|$ markedly differ in intensity and angular distribution. This observation indicates a strong energy dependence of the dynamical parameters that govern the photoionization of the NO D state and is consistent with the existence of a Cooper minimum in the $3p\sigma \rightarrow \epsilon\sigma$ ($l=2$) channel of the ionization continuum.

1. Introduction

Recent advances in experimental technique have allowed the resolution of individual quantum levels of small molecular ions produced by photoionization [1-10]. In particular, optically oriented or aligned diatomic molecules in a specific rovibrational level can now be photoionized using resonance-enhanced multiphoton ionization (REMPI), and the resulting photoelectron angular distributions (PADs) associated with the production of each rovibrational level of the ion can be measured. Although this procedure has been applied so far only to the photoionization of the NO A²Σ⁺ state, such experiments yield a nearly complete description of the photoionization dynamics [6-10]. We report in this Letter the extension of this technique to the photoionization of the NO D²Σ⁺ state.

Photoionization of the NO D²Σ⁺ state has received considerable attention, both experimentally and theoretically [2,11-14]. The first (partially) rotationally resolved photoelectron spectra of the NO

D state were reported by Reilly and co-workers [2] who employed (2+1) REMPI. Using (1+1') REMPI, the same group, in collaboration with McKoy and co-workers [13], also reported rotationally resolved photoelectron spectra of the NO D state as a function of photoelectron kinetic energy; they observed a strong dependence of ion rotational branching ratios on kinetic energy of the photoelectron. They also observed an anomalously large $\Delta N=0$ peak in their experimental spectrum at a photoelectron energy of 330 meV, which they attributed to the 'dynamic' coupling between the NO A²Σ⁺ ($v=4$) and D²Σ⁺ ($v=0$) states. In a subsequent theoretical study, Wang, Stephens, and McKoy [14] attributed the energy dependence of the ion rotational branching ratios and the large $\Delta N=0$ peak observed in photoionization of the NO D state to Cooper minima in the photoionization process.

The Cooper minimum, which is a well-known phenomenon in atomic photoionization [15,16], refers to a vanishing of the electronic dipole matrix element that connects the state being ionized to a partial wave

in the ionization continuum. The possible significance of this energy-dependent dynamical phenomenon in molecular photoionization was first discussed by Chupka [17]. McKoy and co-workers [18] subsequently showed through a series of theoretical calculations that Cooper minima are widespread phenomena in excited-state molecular photoionization. The existence of Cooper minima has been invoked to explain the features in rotationally resolved photoelectron spectra of several molecules, such as the $\text{OH D}^2\Sigma^-$ state [19] and the $\text{NH f}^1\Pi$ state [20]. A Cooper minimum has also been identified in the Rydberg–Rydberg transitions of NO [21].

In the present study, we report rotationally resolved PADs using $(1+1')$ REMPI through the $\text{NO D}^2\Sigma^+$ ($\nu=0$, $N=18$) level. This investigation extends the study of Reilly and co-workers [13]. We probe a photoelectron energy region around 210 meV that differs from that in the previous studies (> 330 meV), and we obtain significantly better photoelectron energy resolution than in earlier work. In addition, the fully rotationally resolved PADs obtained in this study enable us to determine detailed information about photoionization dynamics, including the angle-integrated relative cross section for each ion rotational level.

2. Experimental

The experimental apparatus is described in detail elsewhere [6,7]. Only points pertinent to this experiment are described here. The essence of our time-of-flight (TOF) photoelectron spectrometer is a magnetically shielded, field-free flight tube. The photoelectrons are produced by intersecting a molecular beam of NO with two counterpropagating laser beams at right angles. The photoelectrons ejected in the direction mutually orthogonal to the laser beams and the molecular beam are detected using a microchannel plate located 51 cm from the intersection region.

The two colors λ_1 and λ_2 were generated from Nd:YAG pumped pulsed dye lasers (DCR-1A and PDL-1, GCR-3 and PDL-3; Spectra Physics) operating at a repetition rate of 10 Hz. The excitation color ($\lambda_1=187.1$ nm) was produced by focusing the frequency-doubled output (306.2 nm) of the dye laser (PDL-1) into a hydrogen Raman cell and selecting

the fifth anti-Stokes order using a single-crystal quartz Pellin-Broca prism. More than $15 \mu\text{J}/\text{pulse}$ of 187.1 nm light was obtained by focusing $\approx 11 \text{ mJ}/\text{pulse}$ of 306.2 nm light into the hydrogen Raman cell (80 psi) using a 50 cm focal length lens. The ionization color ($\lambda_2=428$ nm) was obtained from the dye laser (PDL-3) directly. Because the lifetime of the NO D state is approximately 20 ns [22,23], the time delay between the excitation and ionization laser beams was set to be less than 10 ns.

To assign the rotational transitions in the $\text{NO D}^2\Sigma^+-X^2\Pi$ (0–0) band, we performed a wavelength scan in the NO gas cell by collecting the ions produced in the one-color $(1+1)$ REMPI process by λ_1 . As noted earlier [13,24], the gas-cell spectrum obtained near 187 nm is congested because both the $\text{NO D}^2\Sigma^+-X^2\Pi$ (0–0) and the $\text{NO A}^2\Sigma^+-X^2\Pi$ (4–0) vibrational bands appear in this region. The spectrum could be assigned, however, using the known spectroscopic constants of the two transitions [25]. The assignment was further clarified by performing the wavelength scan of a selected region of the spectrum in the photoelectron spectrometer where the above two colors, λ_1 and λ_2 , were used to effect photoionization. In this scan, only photoelectrons produced from the two-color $(1+1')$ REMPI process were collected based on their TOF to obtain the spectrum. Because the photon energy of the second color (λ_2) is well below that needed to ionize the $\text{NO A}^2\Sigma^+$ ($\nu=4$), the spectrum obtained from the photoelectron spectrometer shows only the $\text{NO D}^2\Sigma^+-X^2\Pi$ (0–0) band, thereby facilitating the assignment.

After the spectrum was assigned, the excitation light was tuned to the $Q_{21}+R_1$ (17.5) transition in the $\text{NO D}^2\Sigma^+-X^2\Pi$ (0–0) band to record photoelectron spectra. The energies of the excitation and ionization laser beams were ≈ 300 nJ and $\approx 200 \mu\text{J}$, respectively. Under the conditions in this study, we observed less than 2 photoelectrons per 10 laser shots, and space-charge distortion was negligible. The measurement of photoelectron counts versus excitation and ionization laser powers demonstrated no detectable saturation of either excitation or ionization transitions. Both the excitation and the ionization laser beams were passed through zeroth-order quartz half-wave plates (Special Optics) mounted on stepper-motor-driven rotation stages that allowed independently rotatable polarizations. In the experiment

reported here, the photoelectrons were found to be retarded by ≈ 10 meV caused by stray electric or magnetic fields. This retardation did not affect, however, either the detection efficiency for photoelectrons or the PAD measurements [10]. Our TOF spectrometer gave an energy resolution of ≈ 2 meV, which is sufficient to resolve single rotational levels of NO^+ for values of $N^+ \geq 10$.

Fig. 1 shows a typical photoelectron TOF spectrum. Seven fully resolved photoelectron peaks, which correspond to production of ions in different rotational levels of $\text{NO}^+ X^1\Sigma^+ (v^+=0)$, are clearly discernible. Each peak is denoted by $\Delta N = N^+ - N$, which is the difference between the rotational quantum number of the ion and that of the NO D state. In Fig. 1, the strong asymmetry in intensities for $\Delta N > 0$ and $\Delta N < 0$ transitions with the same $|\Delta N|$ is clearly apparent. This asymmetry cannot be attributed to experimental artifacts such as the change in detection efficiency as a function of photoelectron energy. In Fig. 1, the $\Delta N = +1$ peak is more intense than the $\Delta N = -1$ peak, whereas the reverse is true for the $\Delta N = +3$ peak compared with the $\Delta N = -3$ peak. In the TOF spectrometer, the kinetic energy discrimination of photoelectron detection is most likely against slower photoelectrons. The study of photoelectron counts as a function of photoionization laser wavelength showed, however, no detector bias as the

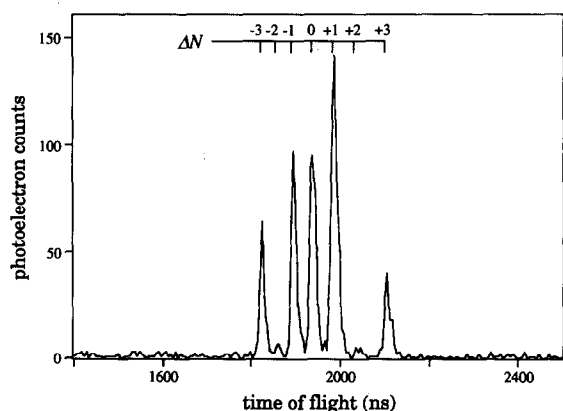


Fig. 1. The time-of-flight photoelectron spectrum of the $(1+1')$ REMPI process $\text{NO } X^2\Pi (v_g=0, J_g=17.5) + h\nu_1 \rightarrow \text{D}^2\Sigma^+ (v=0, N=18) + h\nu_2 \rightarrow \text{NO}^+ X^1\Sigma^+ (v^+=0, N^+) + e^-$. The linear polarization vectors of the excitation and ionization laser beams are parallel to the detection axis so that $\theta=0^\circ$ and $\theta_T=0^\circ$. The full width at half-maximum of each peak is ≈ 2 meV. Here, $\Delta N = N^+ - N$.

photoelectron energy is varied. The study of photoelectron spectra as a function of ionization laser wavelength also showed that the observed photoelectron spectra do not result from sharp autoionization resonances embedded in the ionization continuum. Although we cannot exclude the possibility that broad resonances in the ionization continuum may be excited in the ionization step, we believe that the photoelectron spectrum presented in Fig. 1 is pertinent to the direct photoionization of the NO D state.

The rotationally resolved PADs shown in Fig. 2 were obtained by rotating simultaneously the linear polarization vectors of the excitation and ionization lasers. Each PAD represents the result of 35000 laser shots per waveplate position, i.e. per detection angle θ , and includes nine angles that span two quadrants

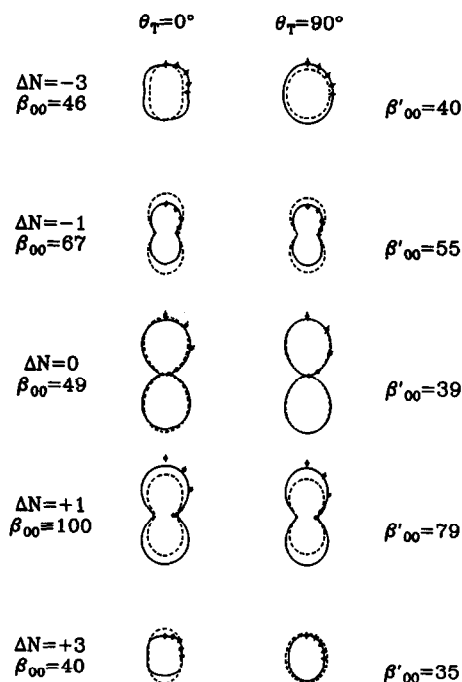


Fig. 2. Polar plots of the PADs for $\theta_T=0^\circ$ and $\theta_T=90^\circ$, in which the linear polarization vector of the ionizing radiation is along the vertical direction. The error bars represent 2σ uncertainties. The solid lines are results of the fit to Eqs. (2) and (4) (see Table 1). The angle-integrated relative cross sections, β_{00} (or β'_{00}), obtained from the fit are listed with the PADs. The dotted lines are results of the nonlinear-least-squares fit to the model under the assumption that the dynamical parameters are energy independent (see text). The scaling of both fit results to the experimental PADs is performed such that the total ionization cross section is equal for all cases.

from 0° to 180° . The experiment was performed with two different angles θ_T held between the excitation- and ionization-laser polarization vectors: $\theta_T=0^\circ$ and $\theta_T=90^\circ$. The symmetry of these experimental geometries dictates that the photoelectron intensities observed at θ and $180^\circ-\theta$ should be the same [26]. The experimentally determined PADs showed, however, that the photoelectron intensities in the second quadrants were up to 10% larger than those in the first quadrants. This difference in intensities can be attributed to systematic errors that result from the imperfect polarization quality of the laser beams and from the minor deviations in the beam paths that arise from rotation of the wave plates [10]. Although great care was taken to reduce these systematic errors, they could not be eliminated entirely in our experiment because we used 187 nm light that is easily absorbed by the optics. To compensate for the observed systematic errors, we averaged the photoelectron intensities at θ and $180^\circ-\theta$ to give a photoelectron intensity at θ (Fig. 2). This procedure did not affect the angle-integrated relative cross section of each ΔN . The error bars in Fig. 2 account for both the background photoelectron counts and the statistical error associated with the photoelectron counting [10].

3. Results and discussion

In Fig. 1 we show a typical two-color TOF photoelectron spectrum obtained by exciting the $Q_{21}+R_1(17.5)$ transition in the $\text{NO } D^2\Sigma^+-X^2\Pi(0-0)$ band. Several salient features are immediately apparent from this spectrum. Seven peaks appear in the spectrum, each of which can be assigned to a single rotational level of the $\text{NO } ^1\Sigma^+(v^+=0)$ ion. The photoelectron spectrum is dominated by $\Delta N=\pm 1$ peaks. The spectrum also shows an intense $\Delta N=0$ peak, $\Delta N=\pm 3$ peaks, and small $\Delta N=\pm 2$ peaks. Within the experimental signal-to-noise ratio, peaks with $|\Delta N|>3$ are not observed. The most striking feature of the spectrum shown in Fig. 1 is the strong asymmetry in intensities of the $\Delta N=+1$ and $\Delta N=-1$ peaks. Similar asymmetry was observed by Song et al. [13] at a somewhat different photoelectron energy of ≈ 330 meV. As described in section 2, this asymmetry cannot be attributed to experimental artifacts. The asymmetry in intensities for the same

$|\Delta N|$ peaks have not been observed in photoionization of the $\text{NO } A^2\Sigma^+$ state, which was extensively studied in our laboratory [6,7,9,10].

The $D^2\Sigma^+(3p\sigma)$ state of NO is the first member of the $n p\sigma$ Rydberg series. According to a quantum-mechanical calculation using the improved virtual orbital method [14], the single-center expansion of the $3p\sigma$ orbital around the center-of-mass of the molecule yields almost pure p character ($\approx 99\%$). Thus, the photoionization selection rule, $l=l_0\pm 1$, for an atomic system where l_0 is a partial-wave component of the Rydberg electron predicts the dominant production of s and d waves in the photoionization process of the NO D state. When this propensity is combined with the photoionization selection rule $\Delta N+l=\text{odd}$, which holds for a $\Sigma-\Sigma$ ionizing transition [27,28], we would expect the appearance of strong $\Delta N=\pm 1$ and $\Delta N=\pm 3$ peaks, as is observed in the experimental photoelectron spectrum. On the other hand, the presence of $\Delta N=0, \pm 2$ peaks associated with the production of odd partial waves in the ionization continuum cannot be explained by the atomlike behavior and clearly indicates the molecular nature of the photoionization process under study. Because the potential that a photoelectron experiences near the molecular ion is not spherically symmetric as in atomic photoionization, the orbital angular momentum quantum number l of the photoelectron is not a good quantum number near the ion-core. For this reason, l -changing collisions between the ion and the photoelectron can occur, producing odd partial waves in the continuum. This simple picture is not sufficient, however, to explain the unusually strong intensity of the $\Delta N=0$ peak [2,11], nor does it address the observed asymmetry in intensities of peaks that have the same value of $|\Delta N|$.

Fig. 2 shows polar plots of experimentally observed PADs associated with each ion rotational state denoted by ΔN for two experimental geometries, $\theta_T=0^\circ$ and $\theta_T=90^\circ$. Also shown in Fig. 2 as solid lines are the linear-least-squares fits of the experimentally observed PADs to the equation

$$I(\theta, \phi; \theta_T) = \beta_{00} Y_{00}(\theta, \phi) + \sum_{L=2,4} \sum_{M=-2}^2 \beta_{LM} Y_{LM}(\theta, \phi). \quad (1)$$

Here $I(\theta, \phi; \theta_T)$ denotes the photoelectron intensity at the polar and azimuthal angle, θ and ϕ , respectively, for a polarization geometry designated by θ_T , and the $Y_{LM}(\theta, \phi)$ are standard spherical harmonic functions. The β_{00} is the angle-integrated relative cross section of each ΔN . The angles θ and ϕ are measured with respect to the Z axis, which is defined to be along the polarization vector of the ionizing light beam, and the detection axis is set to lie in the XZ plane ($\phi=0^\circ$). The drawing of the coordinate frame used in this study can be found in Fig. 1 of Ref. [7]. Eq. (1) is the most general form for PADs that result from the two-photon REMPI under the approximation of weak-field electric-dipole transitions [26]. For the specific experimental geometries employed in this experiment, Eq. (1) reduces to

$$I(\theta, \phi; \theta_T=0^\circ) = \beta_{00} Y_{00}(\theta, \phi) + \beta_{20} Y_{20}(\theta, \phi) + \beta_{40} Y_{40}(\theta, \phi) \quad (2)$$

and

$$I(\theta, \phi; \theta_T=90^\circ) = \beta_{00} Y_{00}(\theta, \phi) + \beta_{20} Y_{20}(\theta, \phi) + \beta_{40} Y_{40}(\theta, \phi) + 2[\beta_{22} Y_{22}(\theta, 0^\circ) + \beta_{42} Y_{42}(\theta, 0^\circ)] \cos(2\phi) \quad (3)$$

Unfortunately, Eq. (3) cannot be used in fitting the PADs obtained with $\theta_T=90^\circ$ because we do not measure the photoelectron intensities as a function of ϕ . At $\phi=0^\circ$, the $Y_{L\pm 2}(\theta, 0^\circ)$ are linearly dependent on the $Y_{L0}(\theta, 0^\circ)$, so all the β_{LM} coefficients in Eq. (3) are impossible to determine uniquely from the fit. Therefore, we fitted the experimental PADs to the following equation [7]:

$$I(\theta, \phi=0; \theta_T=90^\circ) = \beta'_{00} Y_{00}(\theta, 0) + \beta'_{20} Y_{20}(\theta, 0) + \beta'_{40} Y_{40}(\theta, 0) \quad (4)$$

In Eq. (4) β'_{00} does not represent the angle-integrated relative cross section and can be considered only a rough measure of it. The values of β_{LM} (and β'_{LM}) coefficients obtained from the fit are listed in Table 1. Close inspection of experimental PADs and the listed values of β_{LM} (β'_{LM}) in Table 1 clearly shows that the angle-integrated branching ratios for $\Delta N=\pm 1$ and $\Delta N=\pm 3$ transitions differ from each other. The shapes of the PADs that belong to the same $|\Delta N|$ transitions also differ from each other. This

difference is most clearly recognizable from the values of β_{20}/β_{00} (β'_{20}/β'_{00}).

According to the theoretical model developed in this laboratory [9,26], the rotationally resolved PADs depend on the intermediate state alignment, the experimental geometry signified by θ_T , and the parameters that describe the photoionization dynamics. More specifically, the dynamical parameters are magnitudes and phases of the vibrationally averaged radial electric dipole matrix elements that connect the electronic wavefunction of the intermediate state to the outgoing photoelectron partial waves with orbital angular momentum l and the projection of l on the internuclear axis λ . This model, which is built on the theoretical formalism introduced by Dixit and McKoy [29], proved successful in describing the photoionization dynamics of the NO $A^2\Sigma^+$ state [7,9,10]. One critical assumption of this model relevant to the present study is that the dynamical parameters are independent of the photoelectron energy [7,9,10]. The result of this assumption is that, in the high- N limit, the model predicts symmetric intensities and shapes of PADs that correspond to the transitions involving the same $|\Delta N|$. The PADs in Fig. 2, however, are clearly contrary to this prediction and indicate that the assumption of energy-independent dynamical parameters is not satisfactory in the photoionization of the NO $D^2\Sigma^+$ state. The failure of this assumption is dramatically exemplified in Fig. 2. The dotted lines in Fig. 2 are the results of the nonlinear-least-squares fit of experimental PADs to our theoretical model under the assumption that the dynamical parameters are independent of energy. In the fit, the partial wave expansion was cut off at $l=3$ [7], in accordance with the results of the ab initio calculation [14]. As expected, the model fit fails to explain the strong asymmetry observed in intensities and shapes of observed PADs. Because the model fit does not account for the experimental PADs satisfactorily, parameters obtained from the fit are not discussed in this Letter.

The observed asymmetry in intensity and shapes of PADs is rather surprising because the energy span of the photoelectron features observed in this experiment is only 55 meV. The energy difference for photoelectrons associated with $\Delta N=-1$ and $\Delta N=1$ peaks is 18 meV, whereas the ratio of angle-integrated cross sections is almost 2:3 for the same two

Table 1

Results of fitting the β_{LM} to experimental PADs for $(1+1')$ REMPI via the $Q_{21}+R_1(17.5)$ transition to the NO $D^2\Sigma^+$ ($v=0, N=18$) level. Eq. (2) was used for the $\theta_T=0^\circ$ data and Eq. (4) for the $\theta_T=90^\circ$ data. The β_{00} values presented here have been normalized such that $\beta_{00} \equiv 100$ for $\Delta N=1, \theta_T=0^\circ$. The β_{LM} ($L>0$) have been normalized with respect to the β_{00} for each combination of ΔN and θ_T . The values in parentheses represent 1σ uncertainties. The χ^2 values for each linear-least-squares fit are also shown

θ_T	β_{LM}	ΔN						
		-3	-2	-1	0	1	2	3
0°	β_{00}	46(2)	6.2(6)	67(2)	49(2)	100	5.5(6)	40(2)
	β_{20}/β_{00}	0.10(2)	0.08(7)	0.29(2)	0.76(3)	0.58(2)	0.11(8)	0.07(2)
	β_{40}/β_{00}	-0.05(2)	-0.01(7)	-0.00(2)	-0.05(2)	-0.04(1)	-0.03(7)	-0.04(2)
	χ^2	0.01	2.25	1.55	1.92	2.73	1.56	0.78
90°	β'_{00}	40(1)	4.6(6)	55(2)	39(1)	79(2)	4.1(5)	35(1)
	β'_{20}/β'_{00}	0.07(3)	0.15(9)	0.30(2)	0.82(3)	0.56(2)	0.1(1)	0.08(3)
	β'_{40}/β'_{00}	0.00(2)	-0.07(9)	0.00(2)	-0.02(2)	0.00(2)	0.0(1)	0.00(3)
	χ^2	0.23	0.32	0.56	0.58	1.71	4.86	0.36

peaks. Because we ruled out experimentally the possibility that the ionization color, λ_2 , excites sharp autoionization resonances in the ionization continuum, the strong energy dependence of dynamical parameters deduced from rotationally resolved PADs suggests the presence of some other dynamical phenomenon in the ionization continuum.

As noted previously, Wang, Stephens, and McKoy [14] have proposed that Cooper minima exist in the photoionization of the NO $D^2\Sigma^+$ ($3p\sigma$) state. According to this ab initio calculation, the Cooper minima are predicted to occur in the $3p\sigma \rightarrow \epsilon\sigma$ ($l=2$) and $3p\sigma \rightarrow \epsilon\pi$ ($l=2$) channels at photoelectron energies of 0.33 and 3.2 eV, respectively. Considering that photoelectrons observed in this experiment have energies of ≈ 210 meV, it is reasonable to assume that only the Cooper minimum that occurs at 0.33 eV affects the observed photoelectrons significantly. If this Cooper minimum indeed occurs in the continuum, its presence may explain the observed strong energy dependence of dynamical parameters. From our experimental data alone, we are unable to exclude the possibility that perturbation between the levels of the NO $A^2\Sigma^+$ ($v=4$) and $D^2\Sigma^+$ ($v=0$) states also contribute to our observations. The intensity asymmetry between the $\Delta N=1$ and $\Delta N=-1$ peaks strongly suggests, however, the existence of a Cooper minimum in the photoionization dynamics.

The effect of a Cooper minimum in molecular photoionization is difficult, although not impossible, to incorporate into our previous model because the

model is based on the asymptotic partial-wave decomposition of the ionization continuum. Unlike in atomic photoionization, these asymptotic partial-wave channels with orbital angular momentum l are not the eigenchannels near the molecular ion core [30]. Thus, one Cooper minimum can affect both magnitudes and phases of several partial-wave channels through the l mixing in the ionization continuum [31,32].

The fact that we observe strong $\Delta N = \pm 3$ peaks in the photoelectron spectrum is illuminating in the context of the occurrence of the Cooper minimum in the ionization continuum. These peaks result from d partial waves in the ionization continuum that are believed to be the highest even l waves involved in photoionization of the NO $D^2\Sigma^+$ state. In many molecular photoionization studies to date [3,7,33,34], the transitions to the ion rotational states that involve only partial waves with the same l were found to be either very weak or absent. For example, in the photoionization of the $H_2 B^1\Sigma_u^+$ state, the $\Delta J = \pm 3$ transitions were negligible despite the presence of d waves in the ionization continuum [33,34]. In the photoionization of the NO A state studied in this laboratory [7], the $\Delta N = \pm 4$ transitions were absent despite the production of strong f waves. These observations were explained based on the dynamical interference between partial waves with the same l but with different λ that have comparable magnitudes and phases. The observation of the strong $\Delta N = \pm 3$ peaks in this study indicates, however, that

the destructive interference between $d\sigma$ and $d\pi$ waves is suppressed in photoionization of the NO D state. This observation is consistent with the occurrence of a Cooper minimum in the $3p\sigma \rightarrow \epsilon\sigma$ ($l=2$) channel because the smallness of the $d\sigma$ wave compared with the $d\pi$ wave inhibits the destructive interference between $d\sigma$ and $d\pi$ waves, which leads to the large $\Delta N = \pm 3$ peaks.

Whereas the overall physics of the photoionization process seems quite well represented by the ab initio calculations, the comparison between experimentally observed PADs and the theoretically calculated PADs [13,14] reveals a major qualitative discrepancy that cannot be explained by the difference between experiment and ab initio calculations in photoelectron energy or in excitation scheme. In contrast to experiment, the PADs calculated from ab initio theory do not show the observed asymmetry in intensities and angular distributions for the same $|\Delta N|$ peaks. Because the ab initio calculations are based on essentially the same formalism [29] as our model discussed above, the dipole matrix elements that connect the ionizing state to the partial waves in the ionization continuum are the dynamical parameters obtained in the calculations as in our model. Thus, the failure of the ab initio calculations to exhibit the observed asymmetry suggests that they do not correctly reproduce the energy dependence of magnitudes, the phases of dipole matrix elements, or both. Considering the experimental observation that the ratio of angle-integrated cross sections is 2:3 for $\Delta N = -1$ and $\Delta N = 1$ peaks that are only 18 meV apart, the changes in magnitudes of dipole matrix elements with energy alone do not seem to account for the experimental findings because the angle-integrated cross sections roughly scale as the square of the magnitudes of dipole matrix elements. On the other hand, because of the interferences between partial waves, the rotationally resolved PADs are very sensitive to changes in relative phases between dipole matrix elements, which leads us to believe that the energy dependence of phases may explain our experimental observations. We are currently working on obtaining the dynamical parameters for photoionization of the NO D $^2\Sigma^+$ state from refined experiments and a modified model. We believe that the comparison between these quantities and ab initio calculation results will yield valuable information to-

ward the quantitative understanding of photoionization processes for small molecules.

Acknowledgement

We thank D.J. Leahy and F. Merkt for helpful discussions. This work was supported by the National Science Foundation under Grant No. PHY-9320356.

References

- [1] W.G. Wilson, K.S. Viswanathan, E. Sekreta and J.P. Reilly, *J. Phys. Chem.* 88 (1984) 672.
- [2] K.S. Viswanathan, E. Sekreta, E.R. Davidson and J.P. Reilly, *J. Phys. Chem.* 90 (1986) 5078.
- [3] J. Xie and R.N. Zare, *Chem. Phys. Letters* 159 (1989) 399.
- [4] G. Reiser, D. Rieger and K. Müller-Dethlefs, *Chem. Phys. Letters* 183 (1991) 239.
- [5] K. Müller-Dethlefs and E.W. Schlag, *Ann. Rev. Phys. Chem.* 42 (1991) 109, and references therein.
- [6] S.W. Allendorf, D.J. Leahy, D.C. Jacobs and R.N. Zare, *J. Chem. Phys.* 91 (1989) 2216.
- [7] D.J. Leahy, K.L. Reid and R.N. Zare, *J. Chem. Phys.* 95 (1991) 1757.
- [8] K.L. Reid, D.J. Leahy and R.N. Zare, *Phys. Rev. Letters* 68 (1992) 3527.
- [9] D.J. Leahy, K.L. Reid, H. Park and R.N. Zare, *J. Chem. Phys.* 97 (1992) 4948.
- [10] H. Park and R.N. Zare, *J. Chem. Phys.* 99 (1993) 6537.
- [11] H. Rudolph, S.N. Dixit, V. McKoy and W.M. Huo, *Chem. Phys. Letters* 137 (1987) 521.
- [12] H. Rudolph, S.N. Dixit, V. McKoy and W.M. Huo, *J. Chem. Phys.* 88 (1988) 637.
- [13] X. Song, E. Sekreta, J.P. Reilly, H. Rudolph and V. McKoy, *J. Chem. Phys.* 91 (1989) 6062.
- [14] K. Wang, J.A. Stephens and V. McKoy, *J. Chem. Phys.* 95 (1991) 6456.
- [15] U. Fano and J.W. Cooper, *Rev. Mod. Phys.* 40 (1968) 441.
- [16] S.T. Manson, *Phys. Rev. A* 31 (1985) 3698.
- [17] W.A. Chupka, *J. Chem. Phys.* 87 (1987) 1488.
- [18] K. Wang, J.A. Stephens and V. McKoy, *J. Phys. Chem.* 97 (1993) 9874, and references therein.
- [19] E. de Beer, C.A. de Lange, J.A. Stephens, K. Wang and V. McKoy, *J. Chem. Phys.* 95 (1991) 714.
- [20] K. Wang, J.A. Stephens, V. McKoy, E. de Beer, C.A. de Lange and N.P.C. Westwood, *J. Chem. Phys.* 97 (1992) 211.
- [21] S. Fredin, D. Gauyacq, M. Horani, Ch. Jungen, G. Lefevre and F. Masnou-Seeuws, *Mol. Phys.* 60 (1987) 825.
- [22] A.B. Callear, M.J. Pilling and I.W.M. Smith, *Trans. Faraday Soc.* 64 (1968) 2296.
- [23] H. Rottke and H. Zacharias, *J. Chem. Phys.* 83 (1985) 4831.
- [24] G.W. Bethke, *J. Chem. Phys.* 31 (1959) 662.

- [25] K.P. Huber and G. Herzberg, *Molecular spectra and molecular structure, Vol. 4. Constants of diatomic molecules* (Van Nostrand-Reinhold, New York, 1979).
- [26] K.L. Reid, D.J. Leahy and R.N. Zare, *J. Chem. Phys.* 95 (1991) 1746.
- [27] S.N. Dixit and V. McKoy, *Chem. Phys. Letters* 128 (1986) 49.
- [28] J. Xie and R.N. Zare, *J. Chem. Phys.* 93 (1990) 3033.
- [29] S.N. Dixit and V. McKoy, *J. Chem. Phys.* 82 (1985) 3546.
- [30] C.H. Greene and Ch. Jungen, *Advan. At. Mol. Phys.* 21 (1985) 51.
- [31] R.R. Lucchese and V. McKoy, *Phys. Rev. A* 21 (1980) 112.
- [32] J.A. Stephens and V. McKoy, *J. Chem. Phys.* 93 (1990) 7863.
- [33] S.T. Pratt, P.M. Dehmer and J.L. Dehmer, *J. Chem. Phys.* 78 (1983) 4315.
- [34] D.L. Lynch, S.N. Dixit and V. McKoy, *Chem. Phys. Letters* 123 (1986) 315.